Independent and Dependent Scattering in Packed-Sphere Systems

B. L. Drolen* and C. L. Tien†
University of California, Berkeley, California

The present work predicts radiative extinction characteristics of packed-sphere systems; both independent and dependent scattering are considered. This pertains to many radiation and heat transfer applications including packed and fluidized beds, microsphere insulations, and soot or paint layers. Mie scattering theory is used to calculate the independent scattering and absorption coefficients of a packed-sphere system. Radiative transfer predictions based on these coefficients and a simple two-flux model provide much better agreement with reliable experimental data than published ray-tracing and Monte Carlo models. The dependent scattering efficiency is calculated via the form factor technique of X-ray scattering theory, which uses a pair distribution function to correlate the relative positions of the constituent particles in the system. Predictions using two-pair distribution functions, a "modified-liquid" model, and the hard-sphere Percus-Yevick model show excellent agreement with published experimental data.

Nomenclature

a = absorption coefficient
$\bar{a}$ = two-flux absorption parameter
B = slab-geometry back-scatter fraction
c = inter-particle clearance
C = electromagnetic cross-section
D = particle diameter
f_v = particle volume fraction
F = form factor
g = pair distribution function
G = geometric cross section
I = intensity
k = imaginary part of the complex refractive index
L = total thickness of the scattering medium
m = ratio of complex refractive index, $n - ik$, to that of medium
n = real part of complex refractive index
N = number of particles per unit volume or maximum integer count
O_m = position of center of mth particle
p = slab-geometry phase function
Q = efficiency, C/G
r = coordinate for pair distribution function
r_e = electrical resistivity
s = distance traveled into medium
S = $4 \times \sin(\Theta/2)$
T = transmittance or temperature
w = gap size in "liquid" model
x = particle size parameter, $\pi D/\lambda$, or slab coordinate
γ = relative gap size, w/D
ε = emissivity
ζ = $\sqrt{\bar{a}(\bar{a}+2\bar{\sigma})}$
ϑ = polar angle of the plane-parallel slab
Θ = angle between directions of propagation and observation
λ = wavelength
μ = $\cos\vartheta$
ρ = phase shift, $2x|m-1|$
σ = scattering coefficient
$\bar{\sigma}$ = two-flux scattering parameter
φ = azimuthal angle of the plane-parallel slab
Φ = particle scattering phase function
ω = solid angle

Subscripts and Superscripts

a = absorption
b = blackbody
c = critical
D = dependent scattering
e = extinction
i = incoming or incident beam
max = maximum
M = Mie scattering
o = in vacuum
s = scattering
λ = wavelength
ω = directional
$+$ = forward
$-$ = backward

Introduction

RADIATIVE transfer in packed-sphere systems seems to involve complex radiative interactions between the individual spheres due to the close packed environment. This has led many authors to the use of ray-tracing[1,2] and Monte Carlo techniques[3] to incorporate the inter-particle ("dependent") effects. However, from a fundamental standpoint these calculations neglect the effects of particle diffraction and transmission. They are also quite limited in their applicability and are very time consuming. More importantly, it has been shown[4-7] that independent, scattering theory is actually applicable for most packed-sphere systems, and thus their extinction characteristics can be calculated using Mie scattering theory. Figure 1 shows the independent and dependent scattering regimes over a wide range of size parameter, $x = \pi D/\lambda$, and volume fraction, f_v. Zones of x and f_v are also shown, which are representative of typical heat transfer applications.

Mie scattering theory and a two-flux model are used to calculate the extinction coefficients and the transmittance of a packed system of large spheres, $x = \pi D/\lambda \simeq 6500$, for which reliable data are available for comparison in the independent case.[8] The predictions are in better agreement with the data

Received Feb. 24, 1986; revision received May 21, 1986.

*Research Assistant, Department of Mechanical Engineering.
†Professor, Department of Mechanical Engineering. Fellow AIAA.

than those calculated using either ray-tracing or Monte Carlo techniques.

Many studies have shown that dependent scattering decreases the scattering efficiency.[4-7,9-11] This occurs in various packed-sphere systems such as microsphere insulations, deposited soot layers, and paint layers. These dependent effects can be modeled by correlating the relative positions of the scatterers using a pair distribution function, $g(r)$, which represents the probability of finding a neighboring sphere at a distance r from some central sphere. Once these positions are established, the interference of the individual scattered waves can be determined. Previous papers[6,7] illustrate this method using very simple $g(r)$. In this paper several more advanced $g(r)$ are described, including the Percus-Yevick pair distribution function for the hard-sphere potential.[12-15] The predicted dependent scattering efficiencies, using each of these $g(r)$, are compared to reliable experimental data[4,7,11] over a wide range of f_v. The predictions using the Percus-Yevick pair distribution function are in excellent agreement with the data.

Theoretical Background

Consider a radiant beam with intensity $I_{\omega\lambda}$ impinging upon an absorbing, emitting, and scattering packed-sphere system. As this beam traverses the medium, its intensity is attenuated by both the out-scattering of energy into other directions and the absorption of energy by the particles themselves. At the same time, the intensity is enhanced by the in-scattering of radiation from other directions and by the emitted energy from the particles. The variation of intensity in a homogeneous and isotropic medium is quantified by the following equation of transfer[16]:

$$\frac{dI_{\omega\lambda}(s)}{ds} = -a_\lambda I_{\omega\lambda}(s) + a_\lambda I_{\omega\lambda b}[s, T(s)] - \sigma_\lambda I_{\omega\lambda}(s) + \frac{\sigma_\lambda}{4\pi}\int_{4\pi} I_{\omega\lambda}(s)\,\Phi_\lambda(\omega_i \to \omega)\,d\omega_i \quad (1)$$

where $I_{\omega\lambda}$ is the directional spectral intensity, s the distance traveled in the medium, $T(s)$ the temperature at s, and a_λ and σ_λ are the absorption and the scattering coefficients, respectively. Equation (1) also includes the emitted intensity of the particles $I_{\omega\lambda b}$ and the scattering phase function, $\Phi_\lambda(\omega_i \to \omega)$, which represents the scattering from direction ω_i into direction ω and is normalized such that

$$\int_{4\pi} \Phi_\lambda(\omega_i \to \omega)\,d\omega_i = 4\pi \quad (2)$$

The net heat flux is given by the integral of the directional-spectral intensity, weighted by the cosine of the angle between the direction of the flux and the intensity, over all solid angles and wavelengths.[16]

To perform the scattering analysis of a plane-parallel, one-dimensional geometry the particle phase function $\Phi(\Theta)$ must be converted into the proper coordinates for the slab. Note that the angle Θ is relative to a ray incident upon an individual spherical particle and is not the same as ϑ, which is the polar angle of the plane-parallel slab. Given that Θ and ϑ can be related through analytical geometry, assuming azimuthal symmetry, the scattering phase function in the slab geometry can be expressed

$$p(\mu_i, \mu) = \frac{1}{\pi}\int_0^\pi \Phi[\Theta(\mu_i, \varphi_i = 0 \to \mu, \varphi)]\,d\varphi \quad (3)$$

where $\mu = \cos\vartheta$ and

$$\Theta = \cos^{-1}\left[\mu\mu_i + \sqrt{(1-\mu^2)}\sqrt{(1-\mu_i^2)}\cos\varphi\right] \quad (4)$$

The absorption and scattering coefficients in Eq. (1) are defined as the fraction of the total propagating energy that either is scattered out of, or absorbed from a radiant beam per length of travel. They are directly related to the number density of spheres and their effective scattering and absorption cross-sections, $C_{s\lambda}$ and $C_{a\lambda}$ for a packed-sphere system. The sum of the scattering and absorption cross-sections is called the extinction cross-section, $C_{e\lambda}$. These effective areas are a function of the complex refractive index, $m = n - ik$, the particle size parameter and the polarization of the incoming light.[17] Only unpolarized light is considered herein since this is a good approximation for most heat transfer processes.

These cross-sections are nondimensionalized using the physical cross-section, $G = \pi D^2/4$, yielding the scattering, absorption, and extinction efficiencies

$$Q_{s\lambda} = C_{s\lambda}/G; \qquad Q_{a\lambda} = C_{a\lambda}/G; \qquad Q_{e\lambda} = C_{e\lambda}/G \quad (5)$$

The scattering and absorption coefficients are given by

$$\sigma_\lambda = NC_{s\lambda} = GNQ_{s\lambda}; \qquad a_\lambda = NC_{a\lambda} = GNQ_{a\lambda} \quad (6)$$

which can be related to f_v by noticing that for packed-spheres, $N = 6f_v/\pi D^3$. Thus Eq. (6) can be rewritten in terms of f_v and D

$$\sigma_\lambda = \frac{3Q_{s\lambda}f_v}{2D}; \qquad a_\lambda = \frac{3Q_{a\lambda}f_v}{2D} \quad (7)$$

Independent Scattering in Packed-Sphere Systems

Many methods have been used for modeling radiative heat transfer in packed-sphere systems; these include simple geometric methods, ray tracing and Monte Carlo methods, and two-flux methods with either correlated or calculated parameters. These approaches can be categorized in three fundamentally different groups pertaining to the state of the medium, discontinuous (modeled as an idealized geometry), continuous (similar to a participating gas) and pseudo-continuous (a combination of the above).

Discontinuous models treat a packed-sphere system as an idealized geometry (parallel flat plates, close-packed spheres, cubic-packed spheres) and use standard resistance network or layer theory to calculate the heat flux. Vortmeyer[18] published an excellent review of many of the models in this category. Chan and Tien[1] examined a single cubic cell, representative of

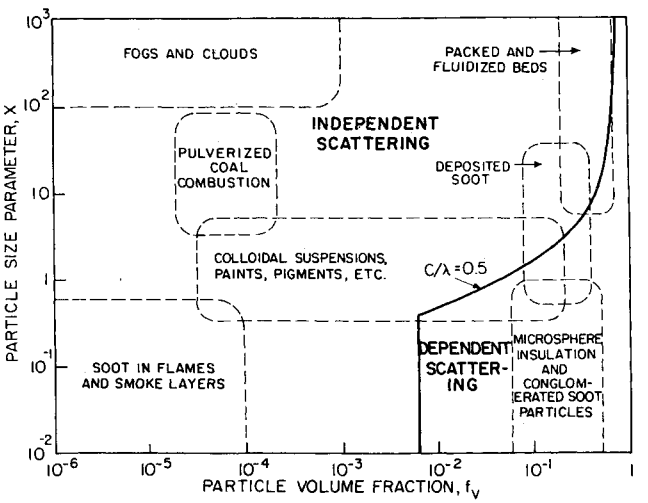

Fig. 1 Independent and dependent scattering regime map: particle size parameter vs volume fraction.

a cubic-packed geometry, and used ray-tracing techniques to calculate the optical properties of a single layer. The transmittance and reflectance of an N-layer bed were then calculated using the net radiation method as is done for multiple-plane windows. Kudo et al.[2] presented a model with variable f_v, which uses a Monte Carlo technique to calculate the reflected, transmitted, and absorbed energy. They examined two different packings, a pyramidal arrangement of four spherical octants, and a cubic cell with sides of length L_c containing a sphere of diameter D at its center ($L_c \geq D$), and suggested that these cases respectively represented dependent and independent scattering.

A truly continuous approach to modeling radiative transfer in packed-sphere systems, though analytically desirable, is clearly inadequate due to the discrete nature of the system. The pseudo-continuous model combines the best aspects of both the continuous and discontinuous models. The particulate medium is modeled as a random distribution of particles of number density N, and the scattering and absorption characteristics of the medium are based on those of the discrete particles. Yang et al.[3] presented a combination ray tracing and Monte Carlo model for packed-bed radiative transfer. They mathematically generated a randomly packed bed of spheres ($f_v = 0.58$) with known sphere center locations. A ray tracing was performed in conjunction with Monte Carlo techniques to determine the extinction characteristics of the packed-sphere system. Brewster and Tien[5] used a simple two-flux approximation to Eq. (1) to predict the transmittance of packed-sphere systems. The solution for the transmittance, assuming a quasi-isotropic phase function with diffuse incident flux and no emission, is given by

$$T = I\frac{(L)}{I_i} = \left[\cosh(\zeta L) + \frac{\bar{\sigma}+\bar{a}}{\zeta}\sinh(\zeta L)\right]^{-1} \tag{8}$$

where I_i is the incident intensity and ζ is given as

$$\zeta = \sqrt{\bar{a}(\bar{a}+2\bar{\sigma})} \tag{9}$$

They derived expressions for $\bar{\sigma}$, $\bar{a}$, and the back-scattering fraction B by integrating the one-dimensional, plane-parallel transfer equation over all solid angles, yielding

$$\bar{\sigma} = 2B\sigma = 3BQ_s f_v/D \tag{10}$$

$$\bar{a} = 2a = 3Q_a f_v/D \tag{11}$$

$$B = \frac{1}{2}\int_0^1\int_{-1}^0 p(\mu,\mu_i)\,d\mu_i\,d\mu \tag{12}$$

They estimated the absorption and scattering efficiencies using the surface emissivity of the spheres and approximated the phase function as that of a diffusely reflecting sphere.[16]

The effects of diffraction and transmission are incorporated in this paper by using the exact Mie scattering solution for the scattering efficiency, the absorption efficiency, and the scattering phase function. These calculations are based on the fundamental properties of the packed-sphere system, namely m, f_v, D, and N. A more general expression for B is given by combining Eq. (3) and Eq. (12)

$$B = \frac{1}{2\pi}\int_0^1\int_{-1}^0\int_0^{\pi}\Phi[\Theta(\mu,\varphi;\mu_i,\varphi_i=0)]\,d\varphi\,d\mu_i\,d\mu \tag{13}$$

The triple integral in Eq. (13) is numerically integrated using twelfth-order Gaussian quadrature and the exact Mie scattering phase function. The integration was checked against specific exact solutions and the results of higher order Gaussian quadrature.

Figure 2 compares the six analytic models that have been discussed to the experimental packed-bed transmittance data of Chen and Churchill.[8] Their widely quoted experiment isolated the radiant mode of heat transfer from the convective and conductive modes. This was achieved by illuminating a bed of spheres (2-16 diam deep) with a modulated, high temperature (700-1366 K), blackbody source and by measuring the transmitted energy via a spectrally independent detector. The experimental data shown is for polished carbon steel spheres, $D = 4.7$ mm and $f_v = 0.60$. The results of Kudo et al.[2] ("dependent") are in poor agreement with the experimental data. The Monte Carlo models which are in closest agreement with the data are those of Yang et al.[3] and Kudo et al.[2] ("independent," $L_c/D = 10$). Of these two models, that of Yang et al.[3] is far more physical since they use $f_v = 0.58$; whereas the model of Kudo et al.[2] effectively uses $f_v = 0.004$, which is clearly inconsistent with the experimental data. Brewster and Tien[5] obtained very good agreement with the experimental data by using $\epsilon = 0.4$, as suggested by Chen and Churchill,[8] and by approximating the phase function as that of a diffusely reflecting large sphere.

Though the predictions obtained by Brewster and Tien[5] are close to the experimental data, Mie scattering calculations improve the results by calculating the extinction coefficients from first principles. The n and k values for steel were approximated using those of iron provided by Siegel and Howell,[16] $n = 1.51$, $k = 1.63$ at $\lambda = 0.589$ μm, scaled to $\lambda_{max} = 2.3$ μm using the Hagen-Rubens formula

$$n \simeq k = \sqrt{0.003\lambda_o/r_e} \tag{14}$$

resulting in $n \simeq k = 3.0$. The size parameter for this calculation, $x = 6505$, is handled readily by the Mie scattering routine of Bohren and Huffman,[17] using double-precision arithmetic and resulting in $Q_a = 0.50$, $Q_s = 1.52$. The value of the back-scattering fraction, B, using Eq. (13) is 0.17. Using Eqs. (10-11) the two-flux parameters are $\bar{\sigma} = 97.7\text{m}^{-1}$ and $\bar{a} = 190.0\text{m}^{-1}$. The figure shows that the results of this approach are in slightly better agreement with the experimental data than the results of Brewster and Tien.[5] In either case, better agreement is achieved at increased packed-bed thickness. This is expected since the pseudo-continuous assumption improves with increasing bed depth. It is somewhat surprising that the

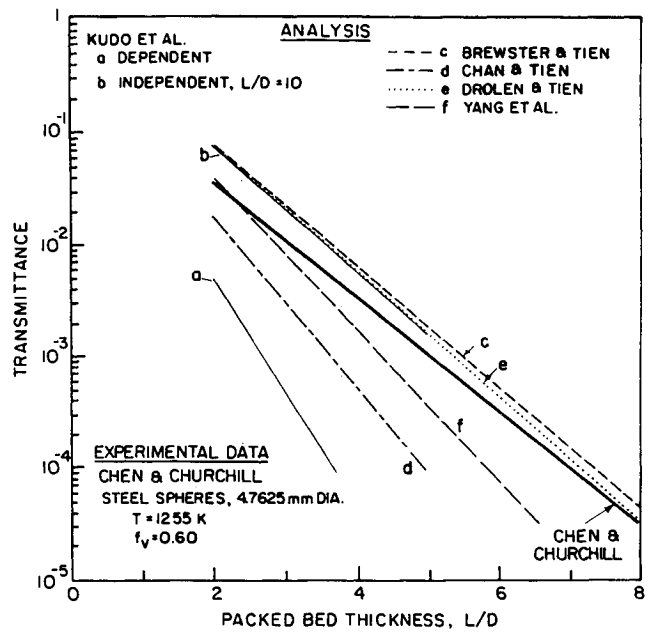

Fig. 2 Transmittance of packed bed of steel spheres vs bed thickness: comparison of experimental data and analytical predictions.

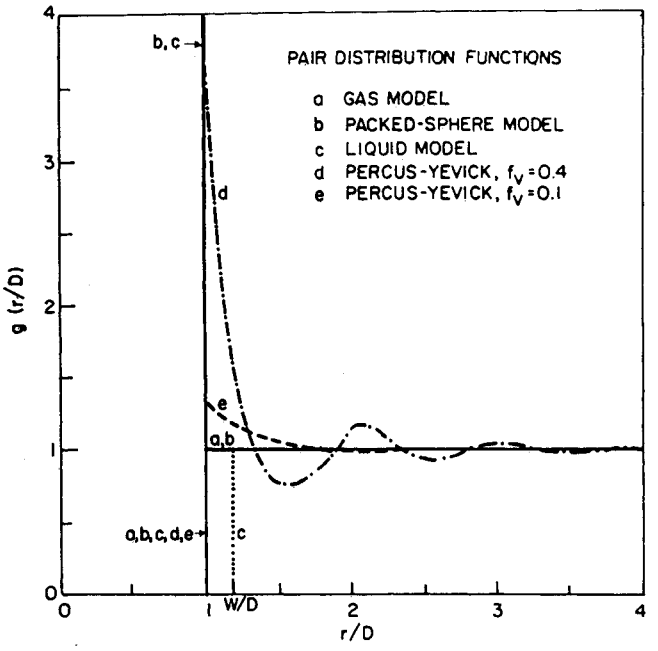

Fig. 3 Four different pair distribution functions plotted with respect to the nondimensional distance from the central scatterer, r/D.

simple two-flux model works so well for the large anisotropic scatterers considered in this study. It is expected that a more robust radiative transfer solution, such as the discrete ordinate method, would further improve the agreement with the data. It is possible that any inaccuracies in the current scattering model are masked by the large value of the absorption coefficient.

Dependent Scattering in Packed-Sphere Systems

Figure 1 shows the distinction between independent and dependent scattering regimes, but what is the significance of the dependent effects and how can the effects be quantified? As early as 1949, workers[9] in the field of paints and pigments published measurements of dependent effects at high f_v. Their data show that as the pigment f_v in a paint layer increases above about 0.3, the "hiding power" (hemispherical reflectance) of the paint layer decreases. The data further demonstrate that this decrease is independent of the thickness of the paint layer and thus is not due to multiple scattering. Many other studies indicate that as f_v increases into the dependent regime, the scattering efficiency decreases from that calculated by Mie scattering theory.[4-7,9-11] Kunitomo et al.[10] inferred a decrease in the scattering efficiency and an increase in the absorption efficiency from diffuse and normal reflectance data for TiO_2 particles in an alkyd resin layer. For x larger than approximately seven, Ishimaru and Kuga[11] measured dependent extinction efficiencies greater than Q_M for $f_v > 0.1$.

To determine the effects of dependent scattering at high f_v, consider a "central" scatterer located at O_m. The interference between the scattered intensity from this particle and the surrounding particles is a function of their relative locations. If the particles move freely about the central scatterer, the system is spherically symmetric and the relative positions depend only on the distance from O_m. The positions of the scatterers in the medium then correlate, via a pair distribution function $g(r)$ as in statistical mechanics. This function represents the likelihood of finding the center of a neighboring particle at some distance r from the central particle.

Most models of dependent scattering follow the form factor approach from X-ray scattering theory to quantify the interference effects. Cartigny et al.[6] gave the following equation for the form factor $F(\Theta)$, which assumes a homogeneous, continuous, isotropic, and infinite distribution of particles

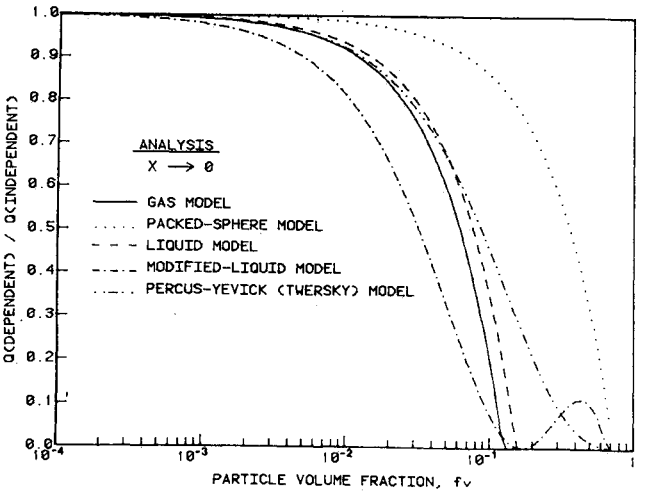

Fig. 4 Reduction in scattering efficiency due to dependent scattering for $x \to 0$.

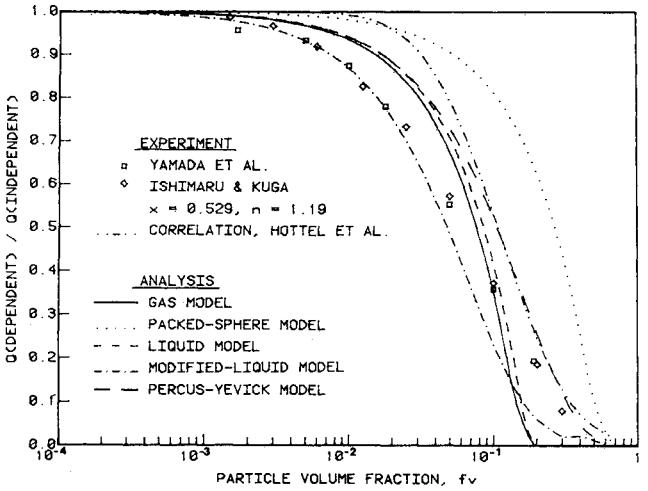

Fig. 5 Reduction in scattering efficiency, at low c/λ (high volume fraction, $x = 0.529$), due to dependent scattering: comparison of experimental data and analytical predictions.

$$F(\Theta) = 1 + 24 f_v \int_0^\infty r^{*2}[g(r^*) - 1]\frac{\sin(Sr^*)}{Sr^*}\,dr^* \quad (15)$$

where $S = 4x\sin(\Theta/2)$, and $r^* = r/D$. Given the form factor, the dependent scattering efficiency for a given particle is calculated

$$\frac{Q_{sD}}{Q_{sM}} = \frac{1}{4\pi}\int_{4\pi} F(\Theta)\,\Phi_M(\Theta)\,d\omega \quad (16)$$

To use any of these equations, a given pair distribution function must be assumed. Figure 3 shows several different pair distribution functions. Cartigny et al.[6] discussed two of these: the "gas" model for low f_v ($f_v < 0.1$) and the "packed-sphere" model for high f_v ($f_v > 0.1$). The "gas" model takes the following form:

$$g(r^*) = 0 \quad \text{for} \quad r^* < 1 \quad (17)$$

$$g(r^*) = 1 \quad \text{for} \quad r^* > 1 \quad (18)$$

Thus, no neighbor exists within one particle diameter of the central scatterer and the likelihood of finding a neighbor outside this diameter is uniform. The "packed-sphere" model

Table 1 Form factor results for various pair distribution functions

Model	$F(\Theta)$
Gas model[6]	$1-8f_v H\left(4x\sin\frac{\Theta}{2}\right)$
Packed-sphere model[6]	$1-8f_v\left[H\left(4x\sin\frac{\Theta}{2}\right)-\left[0.83\sin\left(4x\sin\frac{\Theta}{2}\right)\right]\Big/4x\sin\frac{\Theta}{2}\right]$
Liquid model[15]	$1-8f_v\left[1.64H\left(4.72x\sin\frac{\Theta}{2}\right)-\left[0.83\sin\left(4x\sin\frac{\Theta}{2}\right)\right]\Big/4x\sin\frac{\Theta}{2}\right]$
Modified-liquid model	$1-8f_v\left[\gamma^3 H\left(4\gamma x\sin\frac{\Theta}{2}\right)-\left[0.83\sin\left(4x\sin\frac{\Theta}{2}\right)\right]\Big/4x\sin\frac{\Theta}{2}\right]$
Percus-Yevick hard-sphere model[20]	$\frac{(1-f_v)^4}{(1+2f_v)^2}, \quad x\to 0$
where	$H(U)=\frac{3}{U^3}(\sin U - U\cos U), \quad \gamma = 1\text{-}0.5\exp\left(-\frac{f_v}{0.15}\right)$

attempts to account for the increased f_v by the addition of a Dirac-delta function at $r^*=1$, as shown in Fig. 3, thus

$$g(r^*)=0 \quad \text{for} \quad r^*<1 \tag{19}$$

$$\lim_{\sigma\to 0}\int_{1-\sigma}^{1+\sigma} r^{*2}g(r^*)\,dr^* = \frac{1-3/(4\pi\sqrt{2})}{3} \tag{20}$$

$$g(r^*)=1 \quad \text{for} \quad r^*>1 \tag{21}$$

Gingrich and Warren[19] proposed a "liquid" model which incorporates the "gas" and "packed-sphere" models. They suggested that a gap be inserted between the Dirac-delta function and the uniform distribution. Thus

$$g(r^*)=0 \quad \text{for} \quad r^*<1 \quad \text{and} \quad 1<r^*<\gamma \tag{22}$$

$$\lim_{\sigma\to 0}\int_{1-\sigma}^{1+\sigma} r^{*2}g(r^*)\,dr^* = \frac{1-3/(4\pi\sqrt{2}}{3} \tag{23}$$

$$g(r^*)=1 \quad \text{for} \quad r^*>\gamma \tag{24}$$

This "liquid" model introduces a new parameter, the relative gap size $\gamma = w/D$. Gingrich and Warren[19] suggested that $\gamma = 1.18$ correlates well with their X-ray diffraction data for liquids.

The "liquid" model, Eqs. (22-24), reduces to the "packed-sphere" distribution when $\gamma = 1$. As the gap widens, the results of this model approximate the results of the "gas" model. Therefore, the "gas" and "packed-sphere" models can be effectively combined by allowing the gap in the "liquid" model to be a function of f_v. The following correlation uses this concept to match the data of Yamada et al.[7]

$$\gamma = 1 + 0.5\exp(-6.67f_v) \tag{25}$$

This "modified-liquid" model provides a gradual transition from the "gas" model at low f_v to the "packed-sphere" model at high f_v.

More advanced pair distribution functions have been derived in the study of the statistical mechanics of liquids. Among the best of these is given by the Percus-Yevick (PY) integral equation with the appropriate potential function for particle-particle interactions. For a packed-sphere system, the hard-sphere potential applies, as used in the solutions by Wertheim[12] and Thiele.[13] McQuarrie[14] listed a subroutine for this $g(r^*)$ based on Smith and Henderson's[15] with minor corrections at high f_v behavior. Figure 3 shows the PY pair distribution function for $f_v = 0.4$ and $f_v = 0.1$. In the figure at low f_v the PY $g(r^*)$ approaches the "gas" model. At high f_v it has a sharp peak at $r^*=1$ as does the "packed-sphere" model. It also has the oscillatory behavior that the "liquid" model approximates. The period of oscillation increases with decreasing f_v in the same way the gap of the "modified-liquid" model grows with decreasing f_v. The PY pair distribution function incorporates the behavior of each of the simpler models.

The form factors based on the simpler pair distribution functions, as well as the PY pair distribution function for $x\to 0$ are given in Table 1. The PY form factor for $x>0$ is calculated by performing the integration in Eq. (15) analytically from $r^*=0$ to $r^*=1$ and numerically from $r^*=1$ to $r^*=5$, beyond which $g(r^*)$ is assumed to be one, and the integrand zero. This is a good aproximation for $f_v<0.5$.[15] Q_{sD}/Q_{sM} is determined by numerically integrating Eq. (16). Note that independent of the model chosen, $F\neq f(\Theta)$ for $x\to 0$; therefore Eq. (16) yields

$$Q_{sD}/Q_{sM} = \lim_{x\to 0} F \tag{26}$$

For the PY pair distribution, the reduced scattering efficiency as $x\to 0$ is

$$Q_{sD}/Q_{sM} = (1-f_v)^4/(1+2f_v)^2 \tag{27}$$

as given by Twersky.[20] Figure 4 shows Q_{sD}/Q_{sM} as $x\to 0$ for each of the models discussed. Note that only the PY model behaves reasonably at high f_v.

To verify these dependent scattering models, Fig. 5 compares the models to dependable experimental data for a wide range of f_v and $x=0.529$, $n=1.19$. Hottel et al.[4] published experimental data which led to the widely quoted $c/\lambda_0 = 0.3$ limit. They also correlated their results for $c/\lambda_0 < 0.3$ yielding

$$\log_{10}\log_{10}(Q_{sM}/Q_{sD}) = 0.25 - 5.1c/\lambda_0 \tag{28}$$

The data of both Ishimaru and Kuga[11] and Yamada et al.[7] are included in Fig. 5. Note that the "gas" model works reasonably well for $f_v<0.1$ while the "packed-sphere" model and the PY model are more accurate at higher f_v. The results of the "modified-liquid" model also are shown. Though this "modified-liquid" model is a correlation, it is more fundamental than that of Hottel et al. (Eq. 28).

Ishimaru and Kuga[11] also published dependent scattering results for larger x. Their data for $x=3.518$ and $n=1.19$ are compared in Fig. 6 to each of the analytical models. The PY model predicts the experimental data extremely well while the "gas" and "liquid" models are slightly less accurate. The results of the modified "liquid" model and the "packed-sphere" model are also in reasonable agreement with the data. The PY model is expected to be much more accurate at high f_v; however, due to a lack of data in this region, no conclusive judgement can be made as to the comparative accuracy of the respective models. The results of Hottel's correlation, Eq. (28), are in poor agreement with this large x data. Their correlation is based on experimental data for a limited range of size

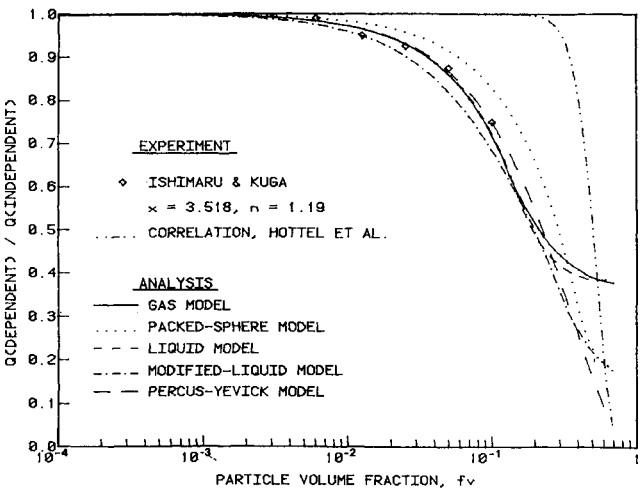

Fig. 6 Reduction in scattering efficiency, at low c/λ (high volume fraction, $x = 3.518$), due to dependent scattering: comparison of experimental data and analytical predictions.

parameter, $0.7 < x < 2.4$ and therefore should not be extended to size parameters outside this range.

Conclusions

Mie scattering results, based on x and m, coupled with a simple two-flux model have been shown in excellent agreement with published experimental data for a packed system of large spheres ($x \simeq 6500$). Furthermore, two-pair distribution functions, the hard-sphere Percus-Yevick model, and a "modified-liquid" model have been used in conjunction with the X-ray scattering form factor technique, to accurately predict the effects of dependent scattering.

References

[1]Chan, C.K. and Tien, C.L., "Radiative Transfer in Packed Spheres," *ASME Journal of Heat Transfer*, Vol. 96, Feb. 1974, pp. 52-58.

[2]Kudo, K., Yang, W.J., Taniguchi, H., and Hayasaka, H., "Radiative Heat Transfer in Packed Spheres by Monte Carlo Method," *U.S.-Japan Heat Transfer Joint Seminar*, Paper J-4, 1985.

[3]Yang, Y.S., Howell, J.R., and Klein, D.E., "Radiative Heat Transfer Through a Randomly Packed Bed of Spheres by the Monte Carlo Method" *ASME Journal of Heat Transfer*, Vol. 105, May 1983, pp. 325-332.

[4]Hottel, H.C., Sarofim, A.F., Dalzell, W.H., and Vasalos, I.A., "Optical Properties of Coatings. Effect of Pigment Concentration," *AIAA Journal*, Vol. 9, Sept. 1971, pp. 1895-1898.

[5]Brewster, M.Q. and Tien, C.L., "Radiative Transfer in Packed/Fluidized Beds: Dependent Versus Independent Scattering," *ASME Journal of Heat Transfer*, Vol. 104, Nov. 1982, pp. 573-579.

[6]Cartigny, J.D., Yamada, Y., and Tien, C.L., "Radiative Transfer with Dependent Scattering by Particles, Part 1: Analytical Investigation," to appear in *ASME Journal of Heat Transfer*.

[7]Yamada, Y., Cartigny, J.D., and Tien, C.L., "Radiative Transfer with Dependent Scattering by Particles, Part 2: Experimental Investigation," to appear in *ASME Journal of Heat Transfer*.

[8]Chen, J.C. and Churchill, S.W., "Radiant Heat Transfer in Packed Beds," *AIChE Journal*, Vol. 9, Jan. 1963, pp. 35-41.

[9]Tinsley, S.G. and Bowman, A., "Rutile Type Titanium Pigments," *Journal of the Oil Colour Chemical Association*, Vol. 32, June 1949, pp. 233-270.

[10]Kunitomo, T., Tsuboi, Y., and Schafey, H.M., "Dependent Scattering and Dependent Absorption of Light in a Fine-Particle Dispersed Medium," *Bulletin of the JSME*, Vol. 28, May 1985, pp. 854-859.

[11]Ishimaru, A. and Kuga, Y., "Attenuation Constant of a Coherent Field in a Dense Distribution of Particles," *Journal of the Optical Society of America*, Vol. 72, Oct. 1982, pp. 1317-1320.

[12]Wertheim, M.S., "Exact Solution of the Percus-Yevick Integral Equation for Hard Spheres," *Physical Review Letters*, Vol. 10, April 1963, pp. 321-323.

[13]Thiele, E., "Equation of State of Hard Spheres," *J. Chem. Phys.*, Vol. 39, July 1963, pp. 474-479.

[14]McQuarrie, D.A., *Statistical Mechanics*, Harper and Row, New York, 1976, Chap. 13, App. D.

[15]Smith, W.R. and Henderson, D., "Analytical Representation of the Percus-Yevick Hard-Sphere Radial Distribution Function," *Molecular Physics*, Vol. 19, Sept. 1970, pp. 411-415.

[16]Siegel, R. and Howell, J.R., *Thermal Radiation Heat Transfer*, 2nd ed., McGraw-Hill, New York, 1981, Chap. 13-20.

[17]Bohren, C.F. and Huffman, D.R., *Absorption and Scattering of Light by Small Particles*, Wiley, New York, 1983.

[18]Vortmeyer, D., "Radiation in Packed Solids," *Sixth International Heat Transfer Conference*, Toronto, Canada, Vol. 6, 1978, pp. 525-539.

[19]Gingrich, N.S. and Warren, B.E., "The Interpretation of X-Ray Diffraction Patterns of a Fluid at Various Densities," *Physical Review*, Vol. 46, Aug. 1934, pp. 248-251.

[20]Twersky, V., "Transparency of Pair-Correlated, Random Distributions of Small Scatterers, with Applications to the Cornea," *Journal of the Optical Society of America*, Vol. 65, May 1975, pp. 524-530.